

Magnetoresistance of Bloch-wall-type magnetic structures induced in NiFe/CoSm exchange-spring bilayers

K. Mibu,* T. Nagahama, and T. Shinjo

Institute for Chemical Research, Kyoto University, Uji, Kyoto-fu 611-0011, Japan

T. Ono

Faculty of Science & Technology, Keio University, 3-14-1 Hiyoshi, Kohoku-ku, Yokohama 223-8522, Japan

(Received 26 February 1998)

The magnetoresistance originating from magnetic structures with gradually rotating magnetic moments, like a Bloch wall, was investigated using soft-magnetic (NiFe)/hard-magnetic (CoSm) bilayers, whose magnetic structures were well characterized. The magnetoresistance was measured with an electric current in the film plane; the magnetoresistance in this geometry corresponds to that due to a current parallel to a Bloch wall. The main feature of the magnetoresistance curves was ruled by the anisotropic magnetoresistance. It was found that a giant magnetoresistance-type effect coexisted; the effect was very small in comparison with the anisotropic magnetoresistance effect. [S0163-1829(98)06934-3]

I. INTRODUCTION

Since the experimental works on Fe whiskers in the 1960's,¹ it has been known that magnetic domain walls contribute to electric resistance in ferromagnetic metals. Cabrera and Falicov first tried to explain this effect theoretically, considering the reflection of conduction electrons by a domain wall,² but the role of a domain wall on electric resistance has not been well elucidated yet. The recent discovery of the giant magnetoresistance (GMR) effect has drawn renewed attention to the magnetoresistance due to a domain wall; Gregg *et al.* have reported that the formation of a stripe domain structure, which has an antiparallel magnetic configuration separated by domain walls, causes an *increase* of resistance due to a "giant magnetoresistive" effect.³ Tataru and Fukuyama, on the other hand, have pointed out, theoretically, that the nucleation of a domain wall in a magnetic wire can cause a *decrease* of resistance when the weak localization is broken by the domain wall.⁴ The latest development of the submicron fabrication technique also has been activating the studies on the effects of domain walls on electric transport properties.^{5,6}

The purpose of the present work is to investigate the magnetoresistance due to magnetic structures with gradually rotating magnetic moments, like a Bloch wall, using a system with well-characterized magnetic structures. Such magnetic structures can be realized in "exchange-spring" multilayers, which consist of soft-magnetic and hard-magnetic layers with an exchange coupling at the interface;⁷⁻⁹ when an inverse magnetic field is applied to the saturated state, the magnetic moments start to rotate at a certain magnetic field, with the directions distributed as a function of the depth from the film surface (Fig. 1). In this paper, we discuss the magnetoresistance with an electric current flowing along the film plane, which corresponds to the magnetoresistance due to an electric current parallel to a Bloch wall. In NiFe/CoSm exchange-spring bilayers, the resistivity of the CoSm layer is about 100 times larger than that of the NiFe layer. Accordingly, when the magnetoresistance is measured in a current-in-plane geometry, the electric current mostly flows in the

NiFe layer that has a twisted magnetic structure in a certain magnetic-field range.

II. EXPERIMENT

The NiFe/CoSm bilayers were prepared on glass substrates. The CoSm layer was made by alternate deposition of Co (5 Å) and Sm (3 Å), and the NiFe layer was deposited from a Ni_{0.8}Fe_{0.2} alloy source at room temperature in a vacuum of 10⁻⁹ Torr range. An external field of 600 Oe was applied in the film plane during the deposition in order to induce a uniaxial magnetic anisotropy in the CoSm film. If CoSm films are deposited at higher substrate temperatures, the coercive force becomes larger on account of crystallization, but the magnetization changes at around zero field because of the coexistence of a minor soft-magnetic phase.⁹ Therefore, amorphouslike CoSm films deposited at room temperature, which showed a square magnetization loop with

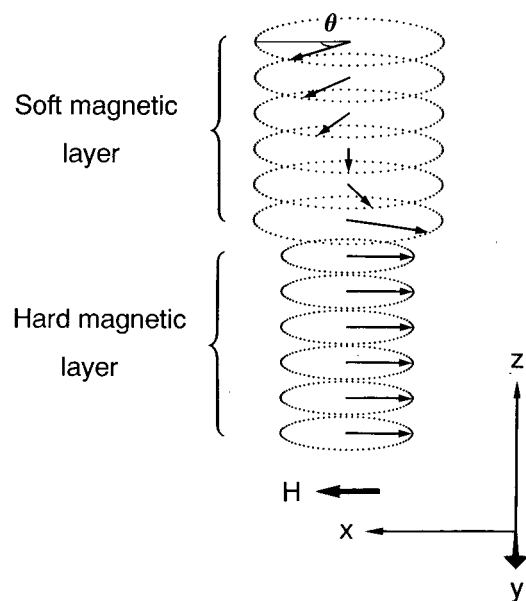


FIG. 1. Illustration of an exchange-spring state in a soft-magnetic/hard-magnetic bilayer.

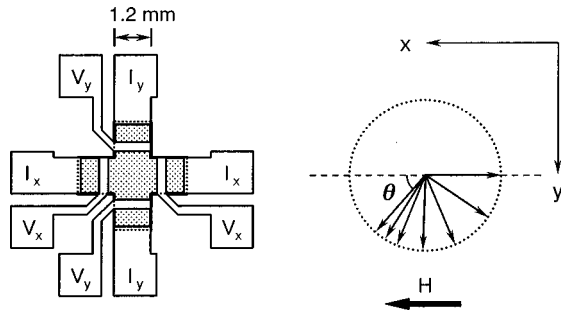


FIG. 2. Configuration for magnetoresistance measurements in two current-in-plane geometries. A cross-shaped bilayer part and two sets of electrodes were deposited on a substrate using different masks, so that the magnetoresistance in two geometries can be measured with the identical sample for the identical magnetic structure.

high remanence ratio, were used as hard-magnetic layers, although the coercive force was not very large.

Magnetoresistance was measured with a magnetic field parallel to the axis of easy magnetization (the x direction in Fig. 1) and with an electric current parallel (ρ_{xx}) and perpendicular (ρ_{yy}) to the magnetic field. A cross-shaped bilayer part and two sets of electrodes were deposited on a substrate using different masks, so that the magnetoresistance in the two geometries can be measured with the identical sample for the identical magnetic structure (Fig. 2). The electric current was set to 5 mA and the direction was switched alternately to measure the resistance for the two directions at each magnetic field.

III. RESULTS AND DISCUSSION

The magnetization curve for a NiFe(300 Å)/CoSm(1000 Å) bilayer at 5.0 K is shown in Fig. 3. When an inverse magnetic field is applied to the saturated state, the magnetic moments start to rotate reversibly at a certain exchange bias field (H_b). When the external field is further increased, a sharp and irreversible magnetization reversal occurs at the field corresponding to the coercive force (H_c), due to the irreversible domain-wall displacement in the CoSm layer. A characteristic reversible magnetization curve is observed between H_b and H_c . The shape of the reversible curve is calculated with a simple atomic layer model.⁸ It is assumed that the bilayer is composed of stacks of atomic layers and that the magnetic moments align ferromagnetically in each

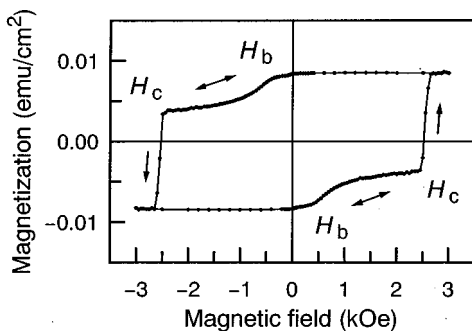


FIG. 3. Magnetization curve of NiFe(300 Å)/CoSm(1000 Å) at 5.0 K. Reversible and irreversible processes are shown by the double-headed and single-headed arrows, respectively.

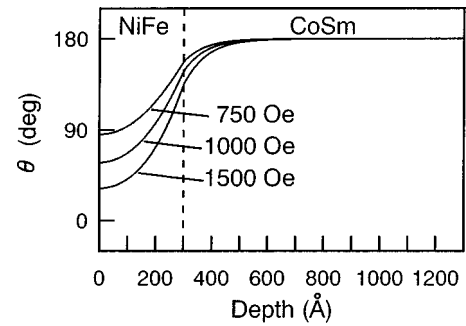


FIG. 4. Calculated distribution of the direction of the magnetic moment in NiFe(300 Å)/CoSm(1000 Å), as a function of the depth from the film surface, at various applied fields. The angle θ is defined as in Figs. 1 and 2.

atomic layer (Fig. 1). Then the total magnetic energy is expressed by the sum of the exchange energy between adjacent atomic layers, the Zeeman energy, and the magnetic anisotropy energy of the atomic layers. The direction of the magnetization for each atomic layer is determined by the condition that gives the minimum in the total magnetic energy. The calculated distribution of the direction of the magnetic moment for NiFe(300 Å)/CoSm(1000 Å), as a function of the depth from the surface, is shown in Fig. 4. The reversible magnetization curve is calculated using the angle distribution obtained for each magnetic field. The calculated curve (Fig. 5) well reproduces the reversible part of the experimental data (Fig. 3).

The magnetoresistance curves of the NiFe(300 Å)/CoSm(1000 Å) bilayer in the two geometries, ρ_{xx} and ρ_{yy} , at 5.0 K are shown in Figs. 6(a) and 6(b). A reversible change is observed in the magnetic-field range where the reversible magnetization process takes place. The observed magnetoresistance shows characteristic field dependence; the resistance changes drastically at around H_b , shows an extremum at around 0.8 kOe, and then recovers gradually. When the magnetic field is increased further, the resistance jumps irreversibly at H_c and reaches the saturation value. The curves measured in the two geometries appear to be a mirror image of each other relative to the average value. The small peaks at around zero field are probably due to a deviation of the magnetic structure from the ideal exchange-spring structure on account of the magnetostatic energy of the cross-shaped sample. [See the small variations in the magnetization curve at around zero field (Fig. 3).]

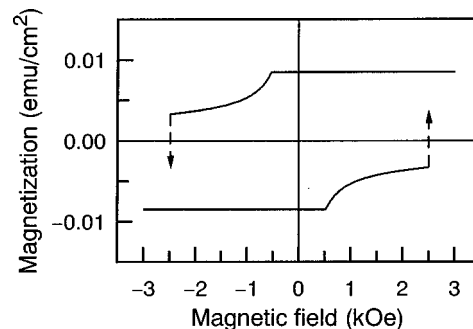


FIG. 5. Calculated reversible magnetization curve for NiFe(300 Å)/CoSm(1000 Å). Irreversible magnetization process takes place in the real sample as shown by the broken arrows.

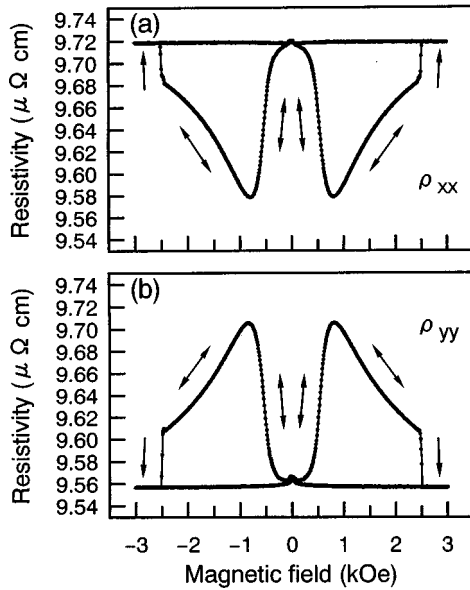


FIG. 6. Magnetoconductance curves of NiFe(300 Å)/CoSm(1000 Å) at 5.0 K; (a) ρ_{xx} and (b) ρ_{yy} . Reversible and irreversible processes are shown by the double-headed and single-headed arrows, respectively.

The fact that the magnetoconductance curves in the two current-in-plane geometries make a mirror image with each other implies that the effect is mainly due to anisotropic magnetoconductance (AMR). Therefore, the AMR effect of the NiFe layer in an exchange-spring state is considered first,⁸ starting from the following phenomenological equations that are valid for uniformly magnetized films:

$$\rho_{xx}^{\text{AMR}} = \rho_{\perp} + (\rho_{\parallel} - \rho_{\perp}) \cos^2 \theta, \quad (1)$$

$$\rho_{yy}^{\text{AMR}} = \rho_{\perp} + (\rho_{\parallel} - \rho_{\perp}) \sin^2 \theta. \quad (2)$$

Here, ρ_{\perp} and ρ_{\parallel} represent the resistivity when the magnetization is perpendicular and parallel to the electric current. The AMR effect can be attributed to the anisotropic electron scattering, whose probability is dependent on the direction of the magnetic moment.¹⁰ In the present system, the direction of the magnetic moment is dependent on the depth from the surface, so that the scattering probability is also. When the mean-free path of conduction electrons is assumed to be short enough in comparison with the thickness of the NiFe layer, the local resistivity (or the inverse of the local conductivity) in the NiFe layer is calculated with the angle distribution in Fig. 4 substituting into Eqs. (1) and (2). The calculated distribution of ρ_{xx}^{AMR} is shown in Fig. 7. In the NiFe layer, the mean-free path is thought to be several tens of Å, so that the distribution in the local resistivity may be somewhat smoothed. In any case, the current direction is kept parallel to the applied electric field, with the current density distributed as a function of the depth from the interface. The AMR of the NiFe layer as a whole is estimated as a parallel circuit of the local resistivity. The calculated resistivity [Figs. 8(a) and 8(b)] well reproduces the feature of the reversible part in the experimental data [Figs. 6(a) and 6(b)]. In this way, the AMR effect makes the dominant contribution

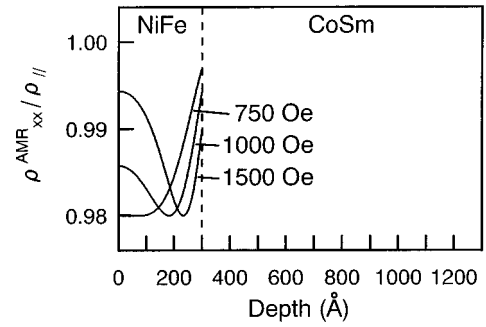


FIG. 7. Calculated distribution of local resistivity (ρ_{xx}^{AMR}) in NiFe(300 Å)/CoSm(1000 Å) at various applied fields. The resistivity in the CoSm layer is not shown since it is about a hundred times larger than that in the NiFe layer.

to the magnetoconductance of a Bloch wall in NiFe, which has a large AMR effect in the bulk, when the current is parallel to the Bloch wall.

The next question is whether there is an additional effect that cannot be explained with the AMR effect. The average of ρ_{xx}^{AMR} and ρ_{yy}^{AMR} in a uniformly magnetized film stays constant at $(\rho_{\parallel} + \rho_{\perp})/2$ independent of the angle θ , as derived from Eqs. (1) and (2). When the average value $\rho_{\text{av}}^{\text{AMR}}$ is calculated for the twisted magnetic structure using the above model, a small amount of negative effect ($\sim 0.005\%$) re-

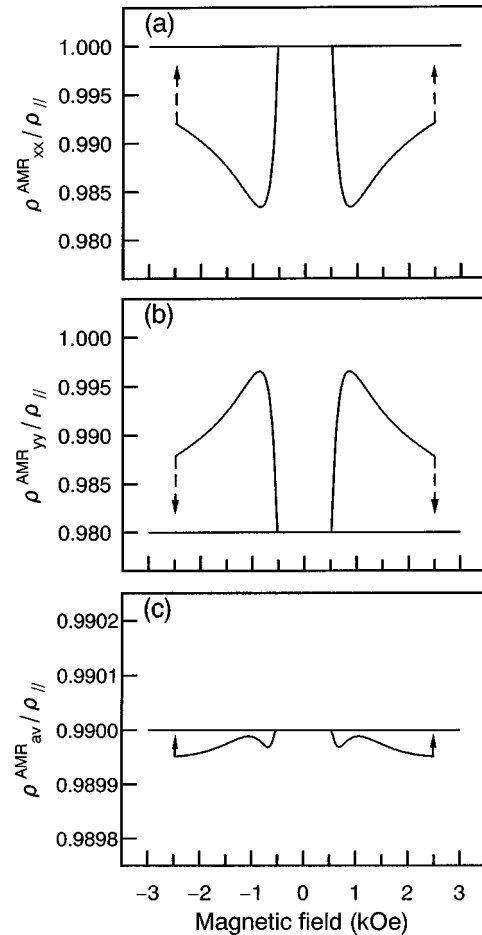


FIG. 8. Calculated AMR curves for NiFe(300 Å)/CoSm(1000 Å); (a) ρ_{xx}^{AMR} , (b) ρ_{yy}^{AMR} , and (c) $\rho_{\text{av}}^{\text{AMR}}$.

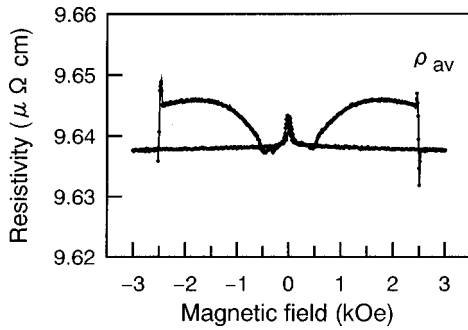


FIG. 9. Average of experimentally obtained ρ_{xx} and ρ_{yy} for NiFe(300 Å)/CoSm(1000 Å) at 5.0 K.

mains on account of the distribution of the current density, as shown in Fig. 8(c). When the mean-free path is larger, the effect in Fig. 8(c) is somewhat smoothed, whereas ρ_{xx}^{AMR} and ρ_{yy}^{AMR} in Figs. 8(a) and 8(b) do not change much. Therefore, if the average of experimentally obtained ρ_{xx} and ρ_{yy} is compared with the calculated average, we can judge whether there is an effect that is not explained with the AMR effect. This can be a better method than the direct comparison of the calculated ρ_{xx}^{AMR} or ρ_{yy}^{AMR} and the experimental ρ_{xx} or ρ_{yy} , since the effect due to a possible small difference between the calculated magnetic structure and the real structure can be canceled. The averaging method of the magnetoresistance measured in two orthogonal geometries has been applied for a single Co or Ni film to study whether the domain walls cause a GMR-type effect.¹¹ In the present study, the magnetic structures of the samples are well characterized, so that the ambiguity in the argument on a small effect derived from the comparison of two large effects is minimized.

The experimental average (ρ_{av}) for NiFe(300 Å)/CoSm(1000 Å) at 5.0 K is shown in Fig. 9. A positive effect of 0.08% was observed in the change of ρ_{av} . This result indicates that a small amount of positive magnetoresistance effect that cannot be explained with the AMR effect is included in the change of ρ_{xx} and ρ_{yy} . The value of ρ_{av} increases as the relative angle between the magnetic moments in the NiFe layer becomes larger, so that this effect is thought to be due to a GMR-type effect, i.e., the effect dependent on the relative configuration of magnetic moments. When the magnetic field becomes larger than about 1.8 kOe, the average magnetoresistance decreases a little. This change can be explained from the calculated directions of the magnetic moments at both interfaces of the NiFe layer, which is shown in Fig. 10. The magnetic moments at both interfaces start to rotate at H_b . The direction at the free interface (θ_f) changes sharply first, and then the change becomes moderate. The direction at the exchange-coupled interface (θ_c), on the other hand, changes rather gradually. As a result, the difference between θ_c and θ_f , which is the measure of the twisted angle in the NiFe layer, changes as shown by the broken line in Fig. 10; it starts to increase when the magnetic field exceeds H_b , reaches the maximum value at around 1.8 kOe, then gradually decreases. It appears that the change in the experimental ρ_{av} reflects this change in the twisted angle. The dependence of the magnetoresistance ratio ($\Delta\rho_{av}$) on the NiFe layer thickness is shown in Fig. 11, for the samples with a NiFe layer thickness of 300 to 1000 Å. The effect was smaller than 0.1% for all the samples measured so far. As the

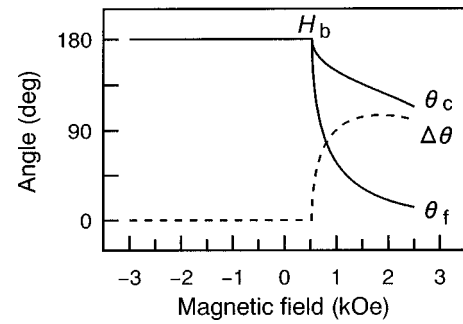


FIG. 10. Calculated direction of the magnetic moment at the free interface (θ_f) and at the exchange-coupled interface (θ_c) of the NiFe layer in NiFe(300 Å)/CoSm(1000 Å) as a function of the applied magnetic field. The difference between θ_c and θ_f , $\Delta\theta$, is also shown by the broken line.

NiFe layer thickness becomes larger, the region where the depth dependence of the direction of the magnetic moment is small increases, so that the magnetoresistance ratio decreases. Recently, Levy and Zhang have pointed out that the introduction of a domain wall mixes the two spin current channels with different resistivity in magnetic metals and causes an increase of the resistance, and estimated the magnetoresistance ratio for the electric current parallel to and perpendicular to the domain wall.¹² The order of the observed positive effect is explainable in the scope of Levy's model. The magnetoresistance ratios at different temperatures are also shown for two samples in Fig. 11. The temperature dependence was not large and the effect was always positive down to 2.0 K. A negative effect accompanied by the nucleation of a domain wall, as reported for a submicron Fe wire by Otani *et al.*,⁶ was not observed in the present system. When the NiFe layer is thick, the influence from the magnetostatic energy becomes relatively large especially at the positions further from the soft/hard interface, so that the magnetic structure deviates from the ideal exchange-spring structure. That makes the extrinsic spikes at around zero field larger, as shown in the preliminary result on NiFe(1000 Å)/CoSm(1000 Å), where an intrinsic positive effect of 0.04% was observed.¹³ Note that we have done the same measurements using samples with several different shapes and sizes, and that it is confirmed that the positive effect is essential in the magnetoresistance of such magnetic structures.

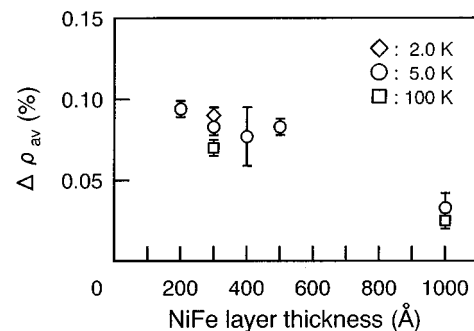


FIG. 11. Magnetoresistance ratio of the GMR-type effect for NiFe(x Å)/CoSm(1000 Å) bilayers with NiFe layer thickness of 300 to 1000 Å at 5.0 K. The results at different temperatures are also shown for two samples.

It is difficult to discuss the GMR-type effect quantitatively, since the magnetoresistance in this configuration cannot be a simple linear combination of the AMR-type and the GMR-type effect. The AMR effect can be excluded when the magnetoresistance is measured with an electric current perpendicular to the film plane (ρ_{zz}), since the angle between the magnetization and the main current direction is 90° at any position. Although the experiment in this geometry is not easy, a preliminary experiment was attempted using bilayers prepared on *V*-groove substrates, and a very small positive magnetoresistance effect was observed.¹⁴

IV. CONCLUSIONS

The magnetoresistance, when the electric current flows in a magnetic film that has a twisted magnetic structure, was studied using NiFe/CoSm exchange-spring bilayers, whose magnetic structures were well characterized. It was found that the magnetoresistance was composed of an AMR-type effect of several % and a GMR-type effect of less than 0.1%.

The results in this work show that (i) the AMR-type effect, i.e., the effect dependent on the direction of magnetization relative to the electric current, is considerably large in a domain wall for the materials that show a large AMR effect in the bulk, and (ii) the GMR-type magnetoresistance, i.e., the effect dependent on the relative configuration of magnetic moments, exists also in the systems with gradually rotating magnetic moments. These results will hence be a guide to discuss further on the magnetoresistance due to domain walls.

ACKNOWLEDGMENTS

The authors would like to thank Dr. N. Hosoito and Mr. S. Hamada for fruitful discussions during this work. This work was partially supported by the New Energy and Industrial Technology Development Organization and the Storage Research Consortium.

*Electronic address: mibu@scl.kyoto-u.ac.jp

¹A. Isin and R. V. Coleman, *Phys. Rev.* **142**, 372 (1966).

²G. G. Cabrera and L. M. Falicov, *Phys. Status Solidi B* **61**, 539 (1974).

³J. F. Gregg, W. Allen, K. Ounadjela, M. Viret, M. Hehn, S. M. Thompson, and J. M. D. Coey, *Phys. Rev. Lett.* **77**, 1580 (1996).

⁴G. Tatara and H. Fukuyama, *Phys. Rev. Lett.* **78**, 3773 (1997).

⁵K. Hong and N. Giordano, *J. Phys.: Condens. Matter* **8**, L301 (1996).

⁶Y. Otani, K. Fukamichi, O. Kitakami, Y. Shimada, B. Pannetier, J. P. Nozieres, T. Matsuda, and A. Tonomura, *Mat. Res. Soc. Symp. Proc.* **475**, 215 (1997).

⁷S. Wüchener, J. Voiron, J. C. Toussaint, and J. J. Préjean, *J. Magn. Magn. Mater.* **148**, 264 (1995).

⁸K. Mibu, T. Nagahama, and T. Shinjo, *J. Magn. Magn. Mater.* **163**, 75 (1996); T. Nagahama, K. Mibu, and T. Shinjo, *J. Phys. D* **31**, 43 (1998).

⁹E. E. Fullerton, J. S. Jiang, M. Grimsditch, C. H. Sowers, and S. D. Bader, *Phys. Rev. B* (to be published).

¹⁰T. R. McGuire and R. I. Potter, *IEEE Trans. Magn.* **MAG-11**, 1018 (1975).

¹¹M. Viret, D. Vignoles, D. Cole, J. M. D. Coey, W. Allen, D. S. Daniel, and J. F. Gregg, *Phys. Rev. B* **53**, 8464 (1996).

¹²P. M. Levy and S. Zhang, *Phys. Rev. Lett.* **79**, 5110 (1997).

¹³K. Mibu, T. Nagahama, T. Ono, and T. Shinjo, *J. Magn. Magn. Mater.* **177-181**, 1267 (1998).

¹⁴T. Nagahama, K. Mibu, T. Ono, and T. Shinjo (unpublished).